

VENTRICULAR FUNCTION

## Left Ventricular Ejection Fraction Calculation from Automatically Selected and Processed Diastolic and Systolic Frames in Short-Axis Cine-MRI

Alain Lalande,<sup>1,\*</sup> N. Salvé,<sup>2</sup> A. Comte,<sup>1</sup> M.-C. Jaulent,<sup>3</sup> L. Legrand,<sup>4</sup>  
P. M. Walker,<sup>1</sup> Y. Cottin,<sup>2</sup> J. E. Wolf,<sup>2</sup> and F. Brunotte<sup>1</sup>

<sup>1</sup>Laboratoire de Biophysique, Faculté de Médecine,  
Université de Bourgogne, Dijon Cedex, France

<sup>2</sup>Service de Cardiologie II, Centre Hospitalier Universitaire de Dijon, Dijon, France

<sup>3</sup>SPIM, INSERM ERM 202, Faculté de Médecine Broussais-Hôtel-Dieu, Paris, France

<sup>4</sup>Laboratoire d'Informatique Médicale, Faculté de Médecine,  
Université de Bourgogne, Dijon, France

### ABSTRACT

The calculation of the left ventricular ejection fraction (LVEF) is dependent upon the accurate measurement of diastolic and systolic left ventricular volumes. Although breath-hold cine magnetic resonance imaging (MRI) allows coverage of the whole cardiac cycle with an excellent time resolution, many authors rely on the visual selection of diastolic and the systolic short-axis slices in order to reduce the postprocessing time. An automatic method was developed to detect the endocardial contour on each image, allowing an automatic selection of the systolic frame. The calculated ejection fraction was compared with radionuclide ventriculography (RNV). Sixty-five patients were examined using an electrocardiogram (ECG)-gated gradient echo sequence. Among these examinations, manual and automatic processing with MRI were compared when the time of the systolic frame concurred. Good correlations have been found between the automatic MRI approach and RNV, and between manual and automatic processing on MRI alone. The results show that the automatic determination of the ejection fraction is feasible, and should constitute an important step toward a larger acceptance of MRI as a routine tool in heart disease imaging. One major benefit of using automatic postprocessing is that it may eliminate the visual choice of the systolic frame, inaccurate in more than 50% of the studied patients.

*Key Words:* Magnetic resonance imaging; Image processing; Left ventricular ejection fraction; Fuzzy logic.

\*Correspondence: Alain Lalande, Laboratoire de Biophysique, Faculté de Médecine, Université de Bourgogne, BP 87900, Dijon Cedex 21079, France; Fax: (33) 3-80-39-32-93; E-mail: alalande@u-bourgogne.fr.

## INTRODUCTION

Left ventricular ejection fraction (LVEF) is one of the most important prognostic indices in coronary artery disease (Multicenter Post Infarction Research Group, 1983). Serial LVEF measurement is widely used for monitoring the cardiac toxicity of anticancer drugs such as anthracyclines (Schwartz et al., 1987). The calculation of the LVEF is dependent upon the accurate measurement of diastolic and systolic volumes of the left ventricle. Although magnetic resonance imaging (MRI) permits these measurements noninvasively, the technique has not yet gained wide acceptance for routinely assessing heart function. One of the major reasons is that dynamic imaging of the heart provides a colossal amount of image data in a single examination. Although the image series covers the whole cardiac cycle, many authors rely on the visual selection of diastolic and the systolic frames in order to reduce the postprocessing time. When using 5 to 10 slice levels, this permits an accurate determination of the volume at diastole and systole and thus yields an estimation of the ejection fraction by manually drawing the endocardial contour. For a heart having suffered an infarct, the wall motion is asynchronous and the visual determination of the diastolic and systolic images becomes precarious.

The aim of this work was to analyze the difference between visually and automatically selected systolic frames in patients with a history of myocardial infarction. The calculated ejection fraction was compared with radionuclide ventriculography (RNV). RNV has the advantage of being directly comparable to magnetic resonance data by providing LVEF based on the volume of the whole left ventricle at each time of the cardiac cycle.

## MATERIALS AND METHODS

### Study Population

Concerning the comparison between automatic processing on MRI and RNV, the study group included 65 patients, 56 males and 9 females with a myocardial infarction. The mean age of the patients was  $58.6 \pm 12.3$  years (range 30–79 years). For the comparison between manual and automatic processing, the study group included 30 patients, 25 males and 5 females, taken among the aforementioned examinations. The mean age of the patients was  $56.9 \pm 14.9$  years (range 30–79 years).

The study was conducted in accordance with the recommendations of the local ethics committee, and informed consent was obtained from each patient.

### Magnetic Resonance Imaging

Magnetic resonance imaging was performed on a 1.5 T magnetic resonance whole body imager (Siemens Magnetom Vision, Siemens GmbH, Erlangen, Germany) using a phased-array receiver coil. The breath-hold cine magnetic resonance data were acquired using an electrocardiogram (ECG)-gated gradient-echo sequence [segmented FLASH two-dimensional (2D) sequence]. The acquisition parameters of this sequence were: repetition time (TR) 9 ms, echo time (TE) 4.4 ms, pulse flip angle  $15^\circ$ , and 9 lines per segment. Multislice contiguous 5-mm section short-axis images were selected perpendicularly to the horizontal long axis from the base to the apex of the left ventricle. A typical patient data set comprised 10 to 15 contiguous slices. According to the breath-holding capability of each patient, the matrix size varied from  $108 \times 256$  to  $144 \times 256$ , therefore requiring 12 to 16 cardiac cycles per slice, i.e., breath holds of 10 to 15 sec. The FOV ranged from 350 to 500 mm. The imaging sequence was implemented with the view sharing technique (Foo et al., 1995), thereby improving the temporal resolution from a nominal 100 ms per frame to 50 ms per frame.

### Radionuclide Ventriculography

All patients underwent radionuclide ventriculography within one week of the MRI examination. The study was carried out with patients in the supine position by using the blood pool labeled with 740 MBq (20 mCi) of  $^{99m}\text{Tc}$ . Thirty-two frames per cardiac cycle were collected on a  $64 \times 64$  matrix and in a left anterior oblique projection with 6 million counts. The resting LVEF was determined by manual definition of diastolic and systolic regions. The background region was manually defined outside the systolic boundary along the lateral wall of the left ventricle.

### Automatic Detection of the Left Ventricle Endocardium from MRI

From MR images, the left ventricle endocardial contour was detected on the whole patient data set, from the most basal slice to the most apical one. For each slice plane, the processing was performed from

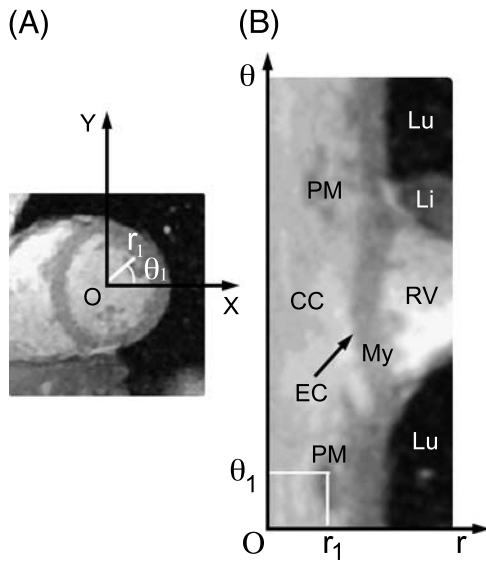


**Figure 1.** Transformation into polar coordinate system. (A) Cartesian coordinates. (B) Polar coordinates. *Abbreviations:* CC=cardiac cavity, My=myocardium, PM=papillary muscles, RV=right ventricle, EC=endocardial contour, Lu=lung, Li=liver.

the image acquired just after the R-wave and covered a substantial part of the cardiac cycle. Once the processing of the frames of a specific slice was completed, the images of the next contiguous slice were processed in a similar fashion. Hence, all the short-axis images of a patient examination are processed, instead of a manual selection of only the images corresponding to diastole and systole. The user intervention is limited to the indication of only one point near the center of the left ventricle on the most basal diastolic slice, at the beginning of the automatic processing. This automatic method to detect the endocardial contour on each image has already been described in previous publications (Lalande et al., 1999) and is presented in the annexe. It is based on fuzzy logic (Jang and Sun, 1995; Mendel, 1995; Zadeh, 1965) and dynamic programming (Lalande et al., 1997; Pope et al., 1985; Thedens et al., 1995). A particularity is the processing in the polar coordinate system rather than in the cartesian coordinate system (Fig. 1), which makes the endocardial contour more or less linear and parallel to the y-axis (Fig. 1B). This makes it easy to exclude of the papillary muscles. Figure 2 shows an example of automatic contouring of a series of images covering the cardiac cycle for a particular slice.

The accuracy of the contour extraction was checked visually. The contours, which appeared to be

erroneous, were traced again, albeit manually. If an aberrant contour appears on one frame, it is usually propagated on the following frames. In such a case, the automatic contour detection was restarted at the image with the aberrant contour after taking the manually traced contour as a new starting point.

### Data Analysis

Left ventricular volumes and the ejection fraction were calculated from the short-axis views. On each image the surface delineated by the left ventricular contour is calculated. For each moment of the cardiac cycle, the left ventricle cavity volume was calculated as the sum of the cavity areas multiplied by the section interval thickness (Cottin et al., 1999). Often, the level of the valves is situated in between two slices. As the extreme basal slice cannot be used for contour determination, the small, but significant distance separating the last usable slice and the level of the valves is taken into account. The missing volume at the base of the ventricle was assumed to be equivalent to a cylinder of an area equal to the surface of the most basal section and a height equal to the distance between this section and the valve plane. Similarly, a correction is performed at the apex of the left ventricle. The missing apical volume was approximated by a semiellipsoid of a short-axis area equal to the surface of the most apical section and a long-axis radius equal to the distance between the most apical section and the cavity extremity. By calculating the left ventricular volume at different phases of the cardiac cycle, left ventricular volume-time curves can be obtained for each patient examination (Fig. 3). The end-diastolic volume (EDV) and the end-systolic volume (ESV) were automatically determined as the maximum and minimum volumes during the cycle (the highest and lowest values on the left ventricular volume-time curve). It is worth noting that the highest volume was not always the volume calculated with the images acquired just after the R-wave.

The LVEF-MRI (%) is calculated as:

$$\text{LVEF - MRI} = 100 \times \frac{\text{EDV} - \text{ESV}}{\text{EDV}} \quad (1)$$

Patient examinations were also processed manually and an experienced observer performed the contouring. Contrary to automatic processing, only the end-diastolic and end-systolic images were manually processed (no left ventricular volume-time curve was constructed). The end-diastolic volume was defined as the volume following the R-wave and the end-systolic

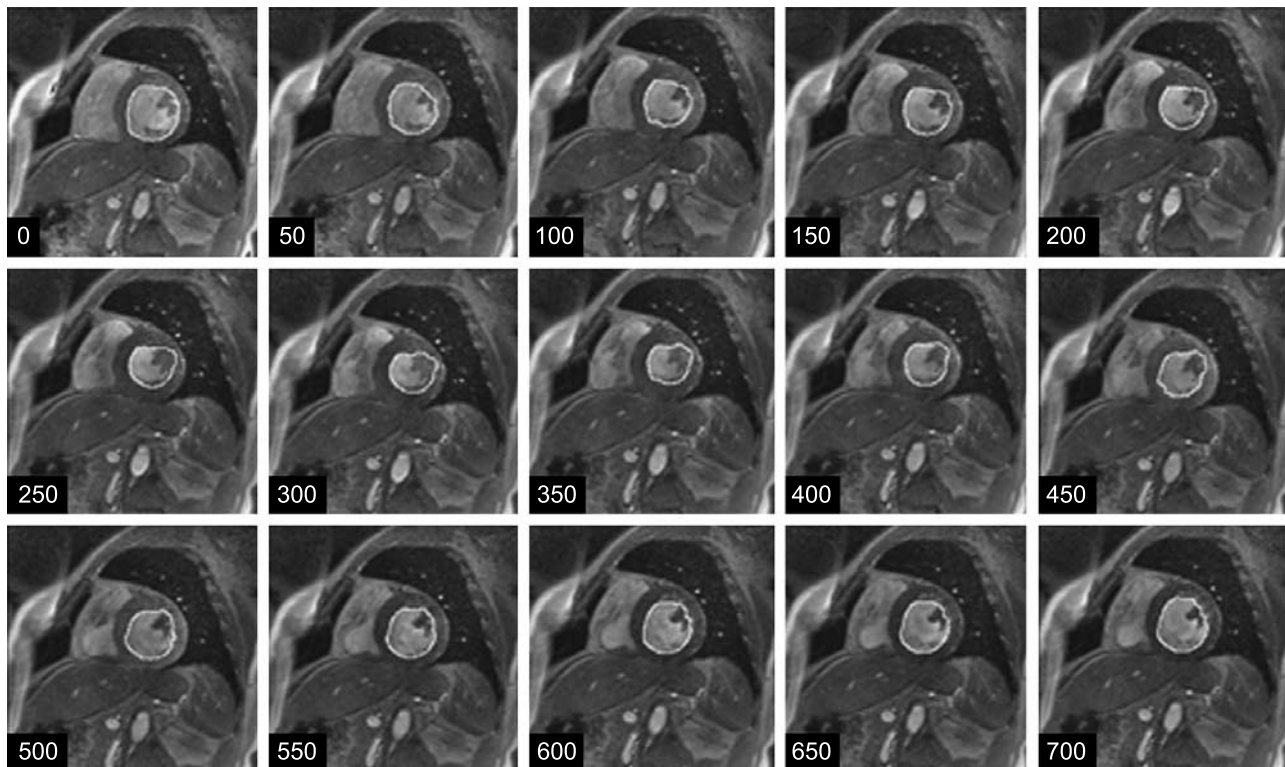


**Figure 2.** Example of automatic detection of endocardial contour on 15 images corresponding to a cardiac cycle for a particular slice. On each image, the bottom left number indicates the time (in msec) after the R-wave.

images were visually chosen as the images with the smallest cavity surface area. Any papillary muscles present in the image were deliberately excluded. The LVEF was calculated using Eq. 1.

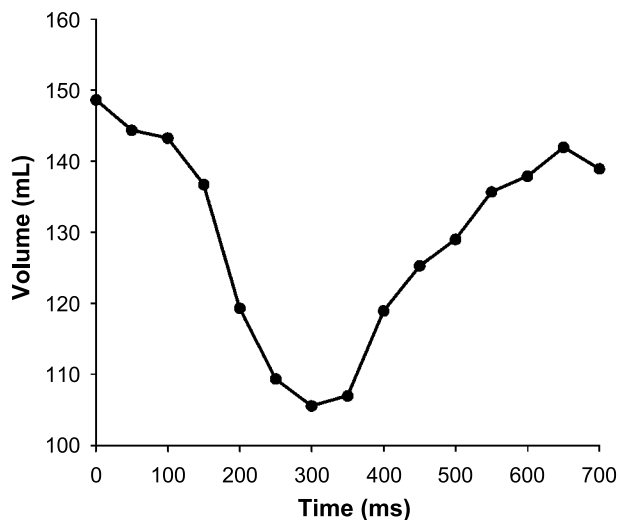


**Figure 3.** Cardiac cavity volume versus time plot.

For all the patient examinations, the LVEF was compared between MRI with automatic postprocessing and RNV.

When the choice of the systolic phase was the same between manual and automatic processing, the LVEF calculated with MRI using the automatic processing method were compared with those calculated from the manually drawn contours. Thirty patient examinations fulfil this condition.

### Statistical Analysis

Comparisons were performed by linear regression analysis and by the Bland-Altman plot (Bland and Altman, 1986). The coefficient of correlation, the linear regression equation, and the standard error of estimate (SEE) were reported. Considering the manual tracing as the independent variable and the automatic contouring as the dependent variable, regression analysis, and Bland-Altman plotting were performed. Regression analysis, and Bland-Altman plotting were also performed by considering RNV as the independent variable, and the automatic postprocessing on MRI as the dependant variable.

**RESULTS**

With respect to the manual processing of the MR images, the inter- and intraobserver variability have already been studied (Cottin et al., 1999).

Contours were manually corrected on  $5.9 \pm 4.1\%$  frames (range 0–16.2%). For the LVEF, a good correlation was found between the MRI automatic method versus radionuclide ventriculography ( $y = 1.03x + 4.8$ ;  $r = 0.88$ ,  $SEE = 5.1$ ) (Fig. 4). When comparing manual

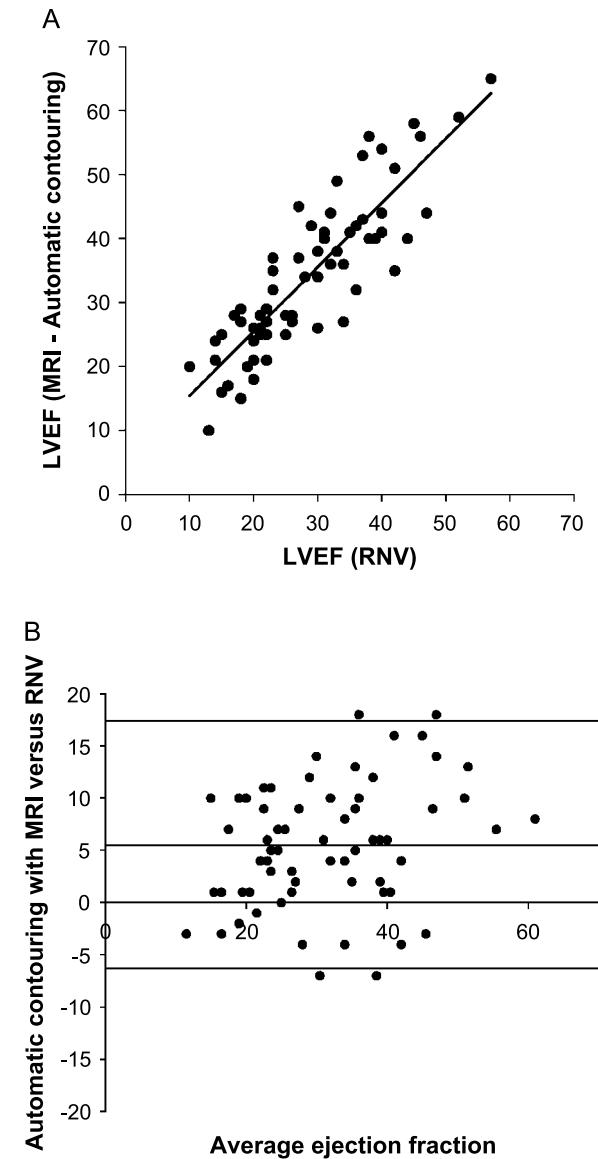


**Figure 4.** (A) Correlation between a LVEF obtained with automatic contouring on MRI and radionuclear ventriculography, and (B) plot of the mean of the LVEF with both techniques against their difference (Bland-Altman plot).

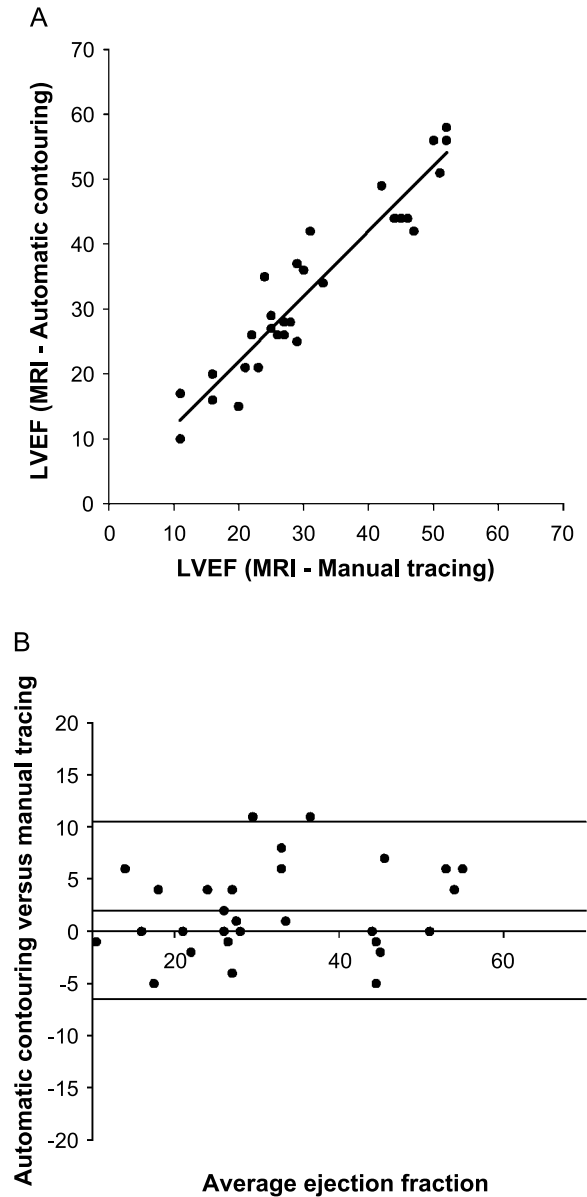


**Figure 5.** (A) Correlation between a LVEF obtained with automatic contouring and manual tracing on MRI when chosen systolic phase is the same, and (B) corresponding plot of the mean of the LVEF with both techniques against their difference (Bland-Altman plot).

and automatic processing, the time of the automatically selected diastolic frame differed by a mean value of less than 2 ms (range 0 to 50 ms) from those defined visually, and by a mean value of 30 ms (range 0 to 150 ms) for the systolic frame. When limiting the comparison to the 30 patients with concordant systolic frames, Fig. 5A shows an excellent correlation ( $y = 0.87x + 1.85$ ;  $r = 0.95$ ;  $SEE = 4.3$ ). The slightly

poorer upslope index (0.87) calculated for the LVEF between automatic and manual contour tracing was essentially due to a lower upslope index (0.82) for the diastolic volume calculation. Indeed, there is an overestimation with manual processing for diastolic volumes greater than 300 mL (7 patient examinations). On the corresponding Bland-Altman plots for the LVEF, the mean difference is  $2.13 \pm 4.30\%$ , indicating that LVEF is slightly overestimated by automatic contouring (Fig. 5B).

## DISCUSSION

The present study has shown that automatic processing of cine-MR data is feasible in routine practice and can yield ejection fraction measurements very close to those of RNV. In fact, no true gold standard exists for the *in vivo* measurement of the left ventricular ejection fraction. Planar gated radionuclide blood-pool ejection fraction has the inconvenience of being dependant on the choice of the best septal projection and on the subtraction of background counts. Radionuclide techniques exhibit a trend toward an underestimation with respect to the X-ray contrast ejection fraction (Folland et al., 1977). Despite these limitations RNV has proven to have a high reproducibility (Wright et al., 2003). In the placebo phase of drug trial reproducibility in RNV was also good (Quaife et al., 1996). The prognostic value of RNV LVEF in patients with coronary artery disease has been established in studies involving thousands of patients (Zaret et al., 1995). Being a count-based technique, the radionuclide method does not depend on the extent and severity of dyskinesia. The fact that the MRI ejection fraction is in strong concordance with planar gated blood-pool ejection fraction is in favor of a similar accuracy for both techniques in patients with coronary artery disease. The correlation with RNV ejection fraction in the patients of the present study is similar to that found by Gaudio et al. (1991) in patients with idiopathic dilated cardiomyopathy. The present method yields satisfactory results in the particular subset of patients with heterogeneous heart contraction.

Manual determination of endocardial contours at diastole and systole is fast and provides an accurate measurement of ejection fraction. Usually the end-diastolic frame is the first image acquired after the R-wave. In the present study, erroneous visual determination of diastole appeared as minimal. On the other hand, end-systole is not accompanied by any reliable wave on the ECG. Mitral valve movements are usually seen only in the long-axis planes and these movements

are not always perfectly visible. Earlier studies have shown that the left ventricular ejection time (LVET) is shortened when the heart rate increases (Leighton et al., 1971). Spontaneous variability of heart rate, arterial blood pressure, venous return, and myocardial contractility may induce variation of LVET (Lewis et al., 1977). As the planes are not imaged simultaneously, slight variations in the duration of systole may occur during the MR examination itself and the systolic time chosen from a given plane may not be valid for the whole data set. Due to contractile asynchrony in coronary artery diseases, the systolic time chosen from wall thickening may also induce errors in systole choice. Asynchrony might reach values as high as 100 ms in patients with impaired left ventricular ejection fraction (<50%) even with a normal QRS duration (Yu et al., 2003). A difference between manual and automatic processing as important as three frames (150 ms) is much more difficult to explain and was found in only a few cases with severe asynchrony and where mitral valve movement was not clearly visible on long-axis views. A difference of one or two images (50 ms to 100 ms) for the systole is easily explained by the aforementioned hypotheses. Studies based on cine-angiography have shown that the end systolic volume is more predictive of the prognosis than end-diastolic volume (White et al., 1987), and so the error due to visual selection of the systolic phase might reduce the reliability of the measured systolic volume. Hence, the visual selection of the systolic images may induce an over-estimation of the systolic volume. This may explain the slight under-estimation of the LVEF calculated by manual tracing versus automatic processing.

The present study was conducted with a time resolution of 50 ms. This time resolution is very close to the 45 ms that has been shown to be adequate for ejection fraction from cine-MRI acquisition in patients studied in the absence of tachycardia (Miller et al., 2002). The present work illustrates that one major advantage of high temporal resolution is the accurate determination of the precise systolic time. The determination of the systolic frame requires the construction of a reliable volume versus time plot. The amount of images to be analyzed (generally more than 200) impedes a manual postprocessing in routine and automatic processing is mandatory.

Several authors have developed algorithms designed on a semiautomatic or automatic delineation of the left ventricular cavity (Baldy et al., 1994; Boudraa, 1997; Fleagle et al., 1991; Furber et al., 1998; Goshtasby and Turner, 1995; Graves et al., 2000; Nachtomly et al., 1998; Ranganath, 1995; Suh et al.,

1993; van der Geest et al., 1997; Waiter et al., 1999; Zimmer and Akselrod, 1996). Some of them use techniques based on geometrical information on pixel groups. In particular, the dynamic contour models (Baldy et al., 1994; Graves et al., 2000; Ranganath, 1995) are dependant upon an energy function. The fitting of a coarse border (defined by the energy function) to the endocardial contour is performed by an iterative deformation process converging to a minimum. The initialization of the coarse border is often manual, at least on the first image of the series of short-axis slices. The application of classic edge operators on preprocessed images has also been widely used. Goshtasby and Turner (1995) used edges as a detection operation, thresholding, and curve fitting techniques. A method presented by Furber et al. (1998) was based on seed growing, differential edge detection and adaptive thresholding. Fleagle et al. (1991) used a series of operators similar to those described by Prewitt. Waiter et al. (1999) developed a semiautomatic method based on first derivative edge detection and weighted polynomial fitting.

From the pixel gray level histogram, it is possible to define the threshold between the myocardium and the blood (Nachatomy et al., 1998). Zimmer and Akselrod (1996) segment the initial image into a three gray-level image (blood, myocardium, and other).

In the method presented by van der Geest et al. (1997), the automatically detected epicardial contour defines a region of interest in which an optimal thresholding allows the detection of the endocardial contour. Pitfalls arise from the detection of epicardial contours.

Many of the proposed methods are semiautomatic and therefore need some manual intervention on each image (Fleagle et al., 1991, 1993; Graves et al., 2000; Waiter et al., 1999; Zimmer and Akselrod, 1996). Moreover, even in the case of well-contrasted images, many of the presented methods are limited by the smooth variation of contrast between blood and the myocardium, which makes the contour uncertain. Indeed, in standard postprocessing approaches, each pixel is supposed to belong to a single area (cavity, myocardium, or endocardial wall), and the contour is ideally a thin line (Kasyhap and Chellappa, 1983). Contrasting with many of the aforementioned processing hypotheses, many pixels belong to several tissues as a consequence of the partial volume effect. Consequently, the contour between the different tissues is rather smoother than the desired sharp transition. Accordingly, automatic cavity contouring based on pixel gray level properties is less reliable. Methods based on fuzzy logic can take into account smooth

contours, tissue heterogeneity, etc. (Keller and Carpenter, 1990). These methods have the key advantage of making the uncertainty of the cardiac contours explicit in algorithm development. The fuzzy C-means model can be used to classify pixels according to their gray level in different predefined classes (or clusters) (Boudraa, 1997). The main drawback of this approach is that the exact number of clusters must be defined before the onset of processing. Our proposed method is not founded upon fuzzy clustering, since the pixels are not classified in predefined classes. Our method is based upon the definition of pixel selection criteria. Suh et al. (1993) proposed a technique using both uncertainty reasoning with fuzzy logic and the Dempster-Shafer theory. Several parameters are calculated for each pixel, based for example on its gray level, the localization of the borders, etc. Contrary to Suh et al., in our method each criterion is represented by a fuzzy set, and the dynamic programming is performed on fuzzy data. The fuzzy set of the cardiac contour points alone does not allow the detection of the endocardial contour. Only the simultaneous use of fuzzy definitions of criteria and dynamic programming allows a correct endocardial contour detection.

Many authors exclude the papillary muscles from the contour (Dulce et al., 1993; Matheijssen et al., 1996; Pattynama et al., 1993). In the present study, the use of dynamic programming with graph searching in polar coordinates allows the exclusion of the papillary muscles on images with relative ease.

In the present study, 6% of the contours had to be manually redrawn. This is a drawback of the presented method and is strongly linked to the insufficient quality of some images. Despite the fact that in most cases the myocardium and the blood pool are sufficiently contrasted in terms of pixel gray level values, flow artifacts due to slow or turbulent blood flow might render the localization of the myocardium wall difficult by reducing the signal of the blood in the vicinity of the endocardium. The improvement of image quality induced by higher cardiac cavity-myocardium contrast in new available sequences (Carr et al., 2001; Merrifield et al., 2001; Moon et al., 2002) may further improve the reliability of fully automatic methods.

## CONCLUSION

For many years, cardiac MRI has been hampered by its low availability and high cost. The automatic determination of the ejection fraction should constitute an important step toward a larger acceptance of MRI as a routine tool in heart disease imaging by reducing the

processing time and reducing operator variability. Foreseeable widespread use of MRI for the study of regional myocardial perfusion and function should contribute to make attractive methods simultaneously allowing the measurement of the left ventricular volume and function. The present study has shown that algorithms derived from the concept of fuzzy logic are well suited to cardiac MR image processing tasks. Although the method described in the present work is not real time, the automatic processing requires less than 10 sec per image on a desktop computer equipped with a 1.2 GHz microprocessor, the user intervention being limited to the indication of only one point near the center of the left ventricle on the first processed image. This study has also highlighted the problem raised by the visual choice of the systolic frame, which might be inaccurate in more than 50% of the studied patients.

#### ANNEXE

The presented automatic contouring method should allow one to process a patient data set and to automatically calculate the ejection fraction. The processing is performed from the most basal slice to the most apical slice. For each slice, it begins with the image acquired just after the R-wave.

All the steps of the automatic endocardial contour detection are illustrated in the flow chart (Fig. 6). For every slice, in order to process the data it is convenient to transpose the image from its original cartesian coordinates into the polar coordinate system. By choosing the center of the left ventricular cavity as the center of the polar coordinate system, the concentric circular form of the myocardium contours produces roughly vertical lines after coordinate transposition. Then, three parameters are defined for each pixel. The first depends upon the pixel gray level value. Indeed, the points of the cardiac contours have roughly the same gray level. Once this gray level, called the reference gray level value, is determined, it is compared with every pixel gray level in the image. The difference between the gray levels defines the first parameter. The second parameter depends on the presence of an edge. It is based on the application of a kernel-based edge operator on the image to detect all the edges. The third parameter modelizes the information retrieved on the previous slice. The contour determined on a slice allows one to define a region of interest for the following slice. In the present context of cardiac image processing, the principal information is the pixel gray level value. The first two parameters, depending directly upon the pixel gray

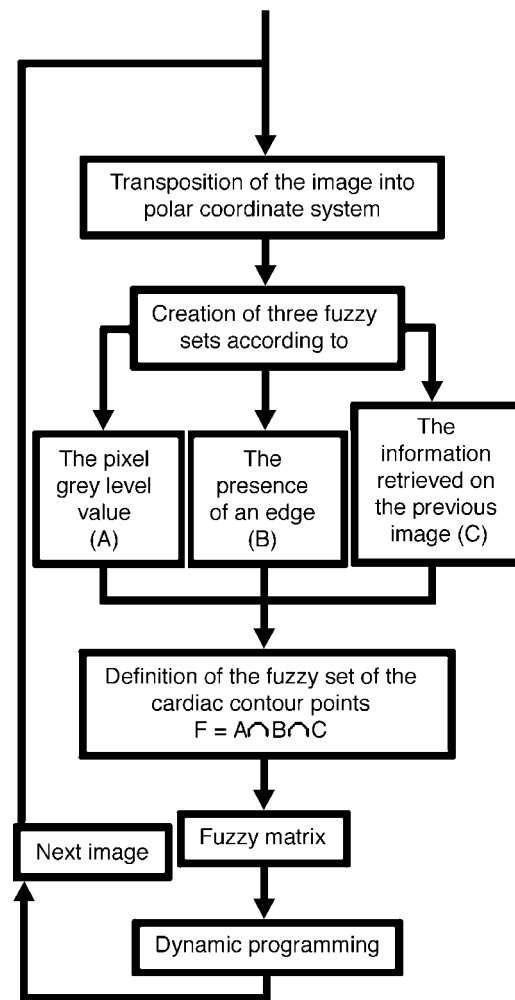


**Figure 6.** Flow diagram summarizing the different steps of the automatic endocardial contour detection performed for every short-axis slice.

level value, are precise but uncertain data. Moreover, we are not sure that the detected contour on a slice is exactly the desired endocardial contour. In order to take into account these uncertainties, a fuzzy set is created for each parameter. The endocardial contour is the class of points that verify a conjunction of the three above criteria. Indeed, the pixels of the endocardial contour have a specific pixel gray level value, belong to an edge, and are enclosed in the region of interest. This class is a fuzzy set whose membership function is given by the minimum of the membership functions of the three criteria. The extent to which a pixel belongs to this fuzzy set is given by its membership degree to this fuzzy set. The data consist of a matrix of membership degrees. The endocardial contour is detected on this fuzzy matrix with the aid of a

dynamic programming technique, called graph searching. The principle difficulty encountered during the endocardial contour detection involves the papillary muscle processing. A modification of the dynamic programming can be made in order to exclude most of the papillary muscles. In practice, in a polar coordinate system, an important deviation of the abscissa of the points detected by graph searching is provoked by the presence of papillary muscles. An interpolation is performed in these areas in order to exclude what is presumed to be the papillary muscle.

### ACKNOWLEDGMENT

This work was supported by a PHRC grant.

### REFERENCES

- Baldy, C., Douek, P., Croisille, P., Magnin, I., Revel, D., Amiel, M. (1994). Automated myocardial edge detection from breath-hold cine-MR images: evaluation of left ventricular volumes and mass. *Magn. Reson. Imaging* 12(4):589–598.
- Bland, J. M., Altman, D. G. (1986). Statistical methods for assessing agreement between two methods of clinical measurements. *Lancet* 13:1294–1300.
- Boudraa, A.-E.-O. (1997). Automated detection of the left ventricular region in magnetic resonance images by Fuzzy C-Means model. *Int. J. Card. Imaging* 13:347–355.
- Carr, J. C., Simonetti, O., Bundy, J., Pereles, S., Finn, J. P. (2001). Cine MR angiography of the heart with segmented true fast imaging with steady state precession. *Radiology* 219(3):828–834.
- Cottin, Y., Touzery, C., Guy, F., Lalande, A., Ressencourt, O., Roy, S., Walker, P. M., Louis, P., Brunotte, F., Wolf, J. E. (1999). MR imaging of the heart in patients after myocardial infarction: effect of increasing intersection gap on measurements of left ventricular volume, ejection fraction, and wall thickness. *Radiology* 213(2):513–520.
- Dulce, M. C., Mostbeck, G. H., Friese, K. K., Caputo, G. R., Higgins, C. B. (1993). Quantification of the left ventricular volumes and function with cine MR imaging: comparison of geometric models with three-dimensional data. *Radiology* 188(2):371–376.
- Fleagle, S. R., Thedens, D. R., Ehrhardt, J. C., Scholz, T. D., Skorton, D. J. (1991). Automated identification of left ventricular borders from spin-echo magnetic resonance images. *Invest. Radiol.* 26:295–303.
- Fleagle, S. R., Thedens, D. R., Stanford, W., Pettigrew, R. I., Reichek, N., Skorton, D. J. (1993). Multicenter trial of automated border detection in cardiac MR imaging. *J. Magn. Reson. Imaging* 3(2):409–415.
- Folland, E. D., Hamilton, G. W., Larson, S. M., Kennedy, J. W., Williams, D. L., Ritchie, J. L. (1977). The radionuclide ejection fraction: a comparison of three radionuclide techniques with contrast angiography. *J. Nucl. Med.* 18:1159–1166.
- Foo, T. K., Bernstein, M. A., Aisen, A. M., Hernandez, R. J., Collick, B. D., Bernstein, T. (1995). Improved ejection fraction and flow velocity estimates with use of view sharing and uniform repetition time excitation with fast cardiac techniques. *Radiology* 195(2):471–478.
- Furber, A., Balzer, P., Cavaró-Ménard, C., Croué, A., Da Costa, E., Lethimonnier, F., Geslin, P., Tadéi, A., Jallet, P., Le Jeune, J.-J. (1998). Experimental validation of an automated edge-detection method for a simultaneous determination of the endocardial and the epicardial borders in short-axis cardiac MR images: application in normal volunteers. *J. Magn. Reson. Imaging* 8(5):1006–1014.
- Gaudio, C., Tanzilli, G., Mazzaroto, P., Motolese, M., Romeo, F., Marino, B., Reale, A. (1991). Comparison of left ventricular ejection fraction by magnetic resonance imaging and radionuclide ventriculography in idiopathic dilated cardiomyopathy. *Am. J. Cardiol.* 67:411–415.
- Goshtasby, A., Turner, D. A. (1995). Segmentation of cardiac cine MR images for extraction of right and left ventricular chamber. *IEEE Trans. Med. Imag.* 14(1):56–64.
- Graves, M. J., Berry, E., Avedisjan, A., Westhead, M., Black, R. T., Beacock, D. J., Kelly, S., Niemi, P. (2000). A multicenter validation of an active contour-based left ventricular analysis technique. *J. Magn. Reson. Imaging* 12:232–239.
- Jang, J.-S. R., Sun, C.-T. (1995). Neuro-fuzzy modeling and control. *Proc. IEEE* 83(3):378–406.
- Kasyhap, R. L., Chellappa, R. (1983). Estimation and choice of neighbours in spatial interaction models of images. *IEEE Trans. Inf. Theory* 29:60–72.
- Keller, J. M., Carpenter, C. L. (1990). Image segmentation in the presence of uncertainty. *Int. J. Intell. Syst.* 5:193–208.
- Lalande, A., Legrand, L., Walker, P. M., Jaulent, M.-C., Guy, F., Cottin, Y., Brunotte, F. (1997). Automatic

- detection of cardiac contours on MR images using fuzzy logic and dynamic programming. *Proc. AMIA Annu. Fall*, 474–478.
- Lalande, A., Legrand, L., Walker, P. M., Guy, F., Cottin, Y., Roy, S., Brunotte, F. (1999). Automatic detection of left ventricular contours from cardiac cine-MRI using fuzzy logic. *Invest. Radiol.* 34:211–217.
- Leighton, R. F., Weissler, A. M., Weinstein, P. B., Wooley, C. F. (1971). Right and left ventricular systolic time intervals. Effects of heart rate, respiration and atrial pacing. *Am. J. Cardiol.* 27:66–72.
- Lewis, R. P., Rittgers, S. E., Forester, W. F., Boudoulas, H. (1977). A critical review of the systolic time intervals. *Circulation* 56:146–158.
- Matheijssen, N. A. A., Baur, L. H. B., Reiber, J. H. C., van der Velde, E. A., van Dijkman, P. R. M., van der Geest, R. J., de Roos, A., van der Wall, E. E. (1996). Assessment of left ventricular volume and mass by cine magnetic resonance imaging in patients with anterior myocardial infarction intra-observer and inter-observer variability on contour detection. *Int. J. Card. Imaging* 12:11–19.
- Mendel, J. M. (1995). Fuzzy logic systems for engineering: a tutorial. *Proc. IEEE* 83(3):345–377.
- Merrifield, R., Keegan, J., Firmin, D., Yang, G.-Z. (2001). Dual contrast TrueFISP imaging for left ventricular segmentation. *Magn. Reson. Med.* 46(5):939–945.
- Miller, S., Simonetti, O. P., Carr, J., Kramer, U., Finn, J. P. (2002). MR Imaging of the heart with cine true fast imaging with steady-state precession: influence of spatial and temporal resolutions on left ventricular functional parameters. *Radiology* 23:263–269.
- Moon, J. C. C., Lorenz, C. H., Francis, J. M., Smith, G. C., Pennell, D. J. (2002). Breath-hold FLASH and FISP cardiovascular MR imaging: left ventricular volume differences and reproducibility. *Radiology* 223:789–797.
- Multicenter Post Infarction Research Group (1983). Risk stratification and survival after myocardial infarction. *N. Engl. J. Med.* 309(6):331–336.
- Nachtomy, E., Cooperstein, R., Vaturi, M., Bosak, E., Vered, Z., Akselrod, S. (1998). Automatic assessment of cardiac function from short-axis MRI: procedure and clinical evaluation. *Magn. Reson. Imaging* 16(4):365–376.
- Pattynama, P. M. T., Lamb, H. J., van der Velde, E. A., van der Wall, E. E., de Roos, A. (1993). Left ventricular measurements with cine and spin-echo MR imaging: a study of reproducibility with variance component analysis. *Radiology* 187(1):261–268.
- Pope, D. L., Parker, D. L., Clayton, P. D., Gustafson, D. E. (1985). Left ventricular border recognition using a dynamic search algorithm. *Radiology* 155(2):513–518.
- Quaife, R. A., Gilbert, E. M., Christian, P. E., Datz, F. L., Mealey, P. C., Volkman, K., Olsen, S. L., Bristow, M. R. (1996). Effects of carvedilol on systolic and diastolic left ventricular performance in idiopathic dilated cardiomyopathy or ischemic cardiomyopathy. *Am. J. Cardiol.* 78:779–784.
- Ranganath, S. (1995). Contour extraction from cardiac MRI studies using snakes. *IEEE Trans. Med. Imag.* 14(2):328–338.
- Schwartz, R. G., McKenzie, W. B., Alexander, J., Sager, P., D'Souza, A., Manatunga, A., Schwartz, P. E., Berger, H. J., Setaro, J., Surkin, L., Wackers, F. J. T., Zaret, B. L. (1987). Congestive heart failure and left ventricular dysfunction complicating doxorubicin therapy. Seven-year experience using serial radionuclide angiocardiology. *Am. J. Med.* 82(6):1109–1118.
- Suh, D. Y., Eisner, R. L., Mersereau, R. M., Pettigrew, R. I. (1993). Knowledge-based system for boundary detection of four-dimensional cardiac magnetic resonance image sequences. *IEEE Trans. Med. Imag.* 12(1):65–72.
- Thekens, D. R., Skorton, D. J., Fleagle, S. R. (1995). Methods of graph searching for border detection in image sequences with applications to cardiac magnetic resonance imaging. *IEEE Trans. Med. Imag.* 14(1):42–55.
- van der Geest, R. J., Buller, V. G. M., Jansen, E., Lamb, H. J., Baur, L. H. B., van der Wall, E. E., de Roos, A., Reiber, J. H. C. (1997). Comparison between manual and semiautomated analysis of left ventricular volume parameters from short-axis MR images. *J. Comput. Assist. Tomogr.* 21(5):756–765.
- Waiter, G. D., McKiddie, F. I., Redpath, T. W., Semple, S. I. K., Trent, R. J. (1999). Determination of normal regional left ventricular function from cine-MR images using a semi-automated edge detection method. *Magn. Reson. Imaging* 17(1):99–107.
- White, H. D., Norris, R. M., Brown, M. A., Brandt, P. W. T., Whitlock, R. M. L., Wild, C. J. (1987). Left ventricular end-systolic volume as the major determinant of survival after recovery from myocardial infarction. *Circulation* 76(1):44–51.
- Wright, G. A., Thackray, S., Howey, S., Cleland, J. G.

- (2003). Left ventricular ejection fraction and volumes from gated blood-pool SPECT: comparison with planar gated blood-pool imaging and assessment of repeatability in patients with heart failure. *J. Nucl. Med.* 44(4):494–498.
- Yu, C. M., Lin, H., Zhang, Q., Sanderson, J. E. (2003). High prevalence of left ventricular systolic and diastolic asynchrony in patients with congestive heart failure and normal QRS duration. *Heart* 89:54–60.
- Zadeh, L. A. (1965). Fuzzy sets. *Inf. Control* 8:338–353.
- Zaret, B. L., Wackers, F. J. T., Terrin, M. L., Forman, S. A., Williams, D. O., Knatterud, G. L., Braunwald, E. (1995). Value of radionuclide rest and exercise left ventricular ejection fraction in assessing survival of patients after thrombolytic therapy for acute myocardial infarction: results of thrombolysis in myocardial infarction (TIMI) phase II study. *J. Am. Coll. Cardiol.* 26(1):73–79.
- Zimmer, Y., Akselrod, S. (1996). An automatic contour extraction algorithm for short-axis cardiac magnetic resonance images. *Med. Phys.* 23(8):1371–1379.

Submitted May 29, 2003

Accepted June 20, 2004